# The Influence of Excess Precipitate on the Non-Ohmic Properties of SnO$_2$-Based Varistors

L.G.P. SIMÕES, P.R. BUENO,* M.O. ORLANDI, E.R. LEITE & E. LONGO

*Interdisciplinary Laboratory of Electrochemistry and Ceramics, Department of Chemistry, Federal University of São Carlos, C. Postal 676, 13565-905—São Carlos, SP, Brazil*

**Abstract.**   Based on our background in the field of nonlinear electrical properties of SnO$_2$-based varistors, we have been observing the influence of microstructural heterogeneities, e.g., the precipitate phase at triple points of the grain boundary region. In this study, we have prepared a SnO$_2$-based varistor system with excess precipitates at triple points in the grain boundary region in order to discuss their influence on the system's non-ohmic properties, including thermal treatment at oxidizing atmospheres. Our results indicate that an excessive amount of such precipitates may be deleterious to the non-ohmic properties because they may create adjacent regions at grain boundaries with lower concentrations of segregated metal atoms, thus increasing the presence of a non-active potential barrier and increasing leakage current paths. Under these circumstances, the effect of thermal treatment in oxidizing atmospheres is to decrease the leakage current density instead of increasing the nonlinear coefficient.

**Keywords:**   varistor, SnO$_2$, precipitate, potential barrier, Mott-Schottky, double-layer

## Introduction

Dense polycrystalline SnO$_2$ systems can be used as a core element of surge absorbers in electronic circuits and as surge arresters in electric power systems [1–7]. The main property for such an application is the nonlinear electrical *I-V* characteristics that can be achieved by densifying SnO$_2$. This densification of SnO$_2$ is high (generally >95%) and can be done by adding CoO, MnO$_2$, ZnO or Bi$_2$O$_3$, for example [8–12]. However, the dense SnO$_2$·CoO systems are the most studied as varistor devices [1–7], presenting high nonlinear coefficient values ($\alpha$) with the addition of small amounts of other oxides, whose metals stabilize in valences of +5 and +3 [1–7], e.g., Nb$_2$O$_5$ and Cr$_2$O$_3$.

Other phases besides the rutile are normally not observed by X-ray diffraction [3–7] and the nonohmic behavior is attributed to grain boundary effects caused by the formation of Schottky-type barriers [1, 13, 14]. Oliveira et al. [15] studied the effect of the addition

of La$_2$O$_3$ to SnO$_2$·CoO·Nb$_2$O$_5$ under different thermal and atmospherical treatments. The results of their work led them to conclude that, under certain circumstances, concentrations of La$_2$O$_3$ higher than 0.05% mol sintered at 1300°C may be deleterious to nonlinear current-voltage characteristics.

In addition, atmospheric treatment can cause important changes in the varistor's nonohmic properties, as reported in references [1–3, 13–15]. The nonlinear electrical properties of varistors can be greatly improved with treatments in oxidizing atmospheres, as discussed in detail in references [1–3, 13, 14].

The main goal of the present work is to discover a relationship between the precipitates present at the grain boundary in triple junction regions of SnO$_2$·CoO-based systems resulting from La$_2$O$_3$ concentrations of over 0.05 mol% and these systems' non-ohmic properties. To this end, we prepared a SnO$_2$·CoO-based varistor with 0.3 mol% of La$_2$O$_3$ sintered at 1300°C. The influence of thermal treatment in an oxidizing atmosphere on the nonlinear *I-V* electrical behavior, allied to a Mott-Schottky analysis and admittance-impedance responses, were used as tools to examine the problem

*To whom all correspondence should be addressed. E-mail: paulo@iris.ufscar.br

and establish the role of precipitates at triple points of the microstructure.

## Experimental Procedure

SnO$_2$ powders were prepared by mechanical mixing in isopropyl alcohol for 6 h, using polypropylene jars with yttrium-stabilized zirconium balls to aid the mixing process. The oxides used were SnO$_2$ (Merck), CoO (Aldrich), Ta$_2$O$_5$ (Aldrich) and La$_2$O$_3$ (Merck), all of them in analytical grade. The composition of the molar system studied was 98.65% SnO$_2$ + 1.0% CoO + 0.05% Ta$_2$O$_5$ + 0.3% La$_2$O$_3$ (SCTL).

The powders were pressed into pellets by uniaxial pressing at 2 MPa, followed by isostatic pressing at 210 MPa. The pellets were then sintered at 1300°C (heating rate of 10°C·min$^{-1}$) for 2 h and cooled to room temperature at a rate of 10°C·min$^{-1}$. The mean grain size was determined by SEM (Scanning Electron Microcopy) analysis (ZEISS microscope Model DSM 940 A) using image analysis software (PGT—IMIX software— ASTM 112 norm). Grain boundary compositions were investigated by EDS (energy dispersive spectroscopy) stage attached to the SEM. The relative densities of the samples were measured using the Archimedes method. The rutile tetragonal structure of SnO$_2$ was confirmed by X-ray diffraction (SIEMENS Model D-5000).

For the electrical measurements, silver contacts were painted on the samples' surfaces and then treated at 400°C for 30 min. Current-voltage measurements were taken using a high voltage measure unit (KEITHLEY Model 237). The impedance measurements were taken with a frequency response analyzer (HP 4194 A) at frequencies ranging from 100 Hz to 15 MHz, with a voltage amplitude of 0.5 V. The bias voltage was measured from 0 to 38 V.

## Results and Discussion

Figure 1 shows X-ray diffraction pattern of the SCTL system that evidences the presence of only a single rutile phase. As already discussed in other papers [2–7, 15], the use of X-ray diffraction patterns does not allow for the identification of phases other than rutile, because the precipitate phases existing in the grain boundary region are present in amounts below 0.5%. Figure 2 shows a SEM micrograph demonstrating that the SCTL
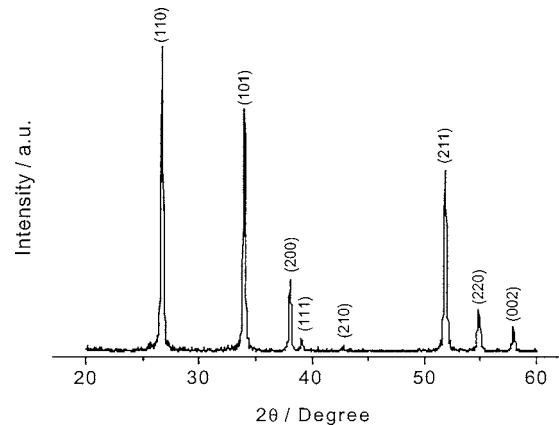


*Fig. 1.* X-ray diffraction pattern of the SnO$_2$·CoO-based system studied.

system is denser (97% of theoretical density) and more homogeneous than the ZnO·Bi$_2$O$_3$-based varistor system. However, precipitates in the grain boundary region become visible through SEM micrography, especially at triple points between grains. The EDS analysis shows that precipitate phases are rich in cobalt and oxygen atoms. This result is very important and will be discussed later herein.

A plot of the *I-V* characteristics for the SCTL system is presented in Fig. 3, which reveals the *I-V* plots in two different situations. The first one is the response of SCTL to sintering and the other one is after a heat treatment in an oxygen-rich atmosphere similar to that reported in [1, 2, 13, 14]. Table 1 lists the nonlinear coefficient ($\alpha$), breakdown voltage ($E_b$), mean grain size and leakage current values before and after thermal heat treatment in an oxidizing-rich atmosphere.

Regarding the results listed in Table 1, it is important to note that the oxidizing-rich atmosphere has no strong effect on the $\alpha$ value, as is the case with other systems reported on in literature [1, 2, 13–15], although the leakage current dropped to half of its original value and

*Table 1.* Nonlinear coefficient ($\alpha$), breakdown voltage ($E_b$), mean grain size and leakage current values for the SnO$_2$·CoO-based system studied.

|  | $\alpha$ | $E_b$ (V·cm$^{-1}$) | Leakage current ($\mu$A) | Mean grain size ($\mu$m) |
|---|---|---|---|---|
| As sintered | 12 | 6000 | 188 | 2.60 |
| After O$_2$ rich atmosphere treatment | 15 | 6300 | 94 | 2.58 |
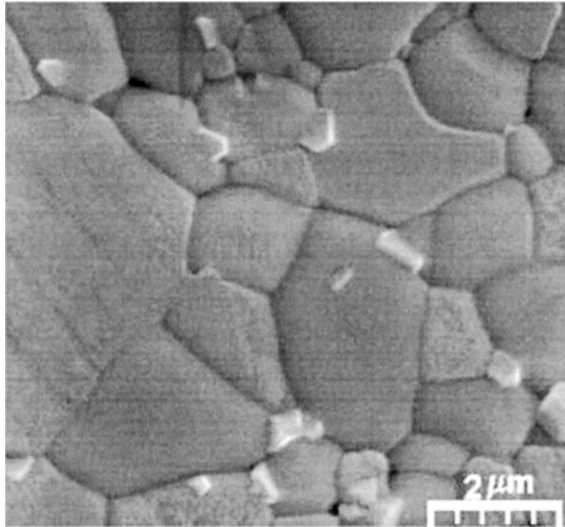
(a)
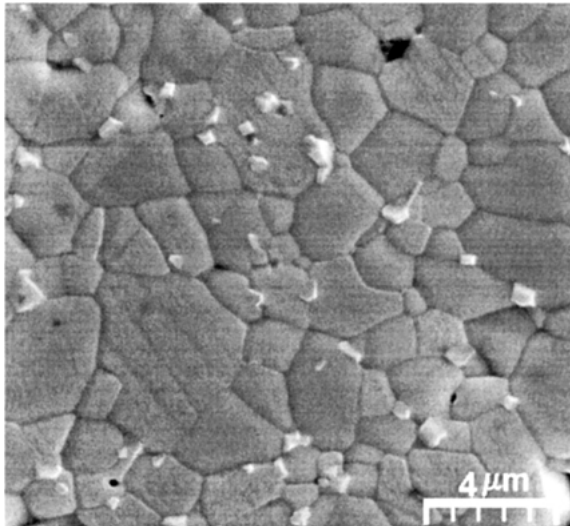


(b)

*Fig. 2.* SEM micrographs of the $SnO_2 \cdot CoO$-based system showing the excess of precipitates at triple points of the grain boundary region.



*Fig. 3.* *I-V* characteristics of the $SnO_2 \cdot CoO$-based varistor system. (○) As-sintered and ( ) after thermal treatment in an oxygen-rich atmosphere.

the breakdown voltage increased, as expected from the model proposed in Ref. [1].

To understand this result, is important to be familiar with the microstructural characteristics of the sample studied here. According to the model presented in reference ([1], 4/id), the non-ohmic properties are improved by the enrichment of grain boundaries with oxygen species, which improves the "*p*-type characteristics" of
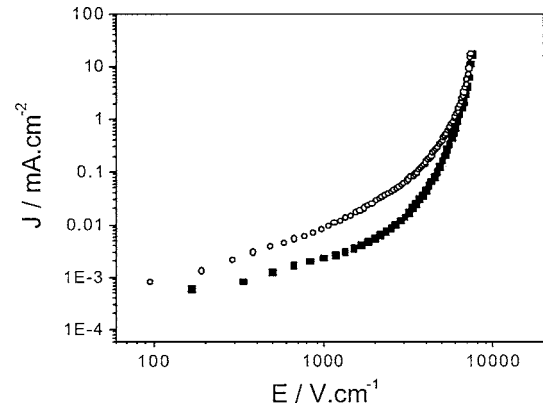
the grain boundaries. Nevertheless, it is very important to distinguish segregate metal atoms (possibly forming a metal oxide region with few atomic layers thick) at grain boundaries from precipitate phases, at triple points, such as the one presented in Fig. 2, which was verified by EDS as being rich in cobalt and oxygen elements (the metal atoms segregated at grain boundaries are responsible for the potential barriers between adjacent grain, while the precipitate phase at triple points only increases the local concentration of metal oxides). Although both segregates and precipitates phases can be enriched by oxygen species, what determines the non-ohmic varistor properties is only the active potential barrier related to metals with *p*-type characteristics segregated at grain boundaries (once this phase does not form potential barriers, the enrichment of precipitate phase locating at triple points of microstructure does not change the electrical features of the system). In other words, the active potential barriers are formed of grain-grain type junctions ($SnO_2-SnO_2$) having segregated metal atoms between them. Upon oxidation, these metals form *p*-type metal oxides, whose acceptor states that are responsible for activating the potential barriers.

Therefore, when precipitates are present in higher concentrations at triple points, as in the present case, due to the addition of 0.3% of $La_2O_3$ (note from another paper that 0.05% suffices to achieve good non-ohmic properties in systems sintered at $1300°C$) [15], they can affect the nature of $SnO_2-SnO_2$ junctions and, hence, the number of active barriers. Once the precipitates are present in triple junctions of the microstructure,

they can cause adjacent $SnO_2$—$SnO_2$ junctions poor in segregated metal atoms because precipitates consume the segregated metal atoms in regions adjacent to them. Such adjacent regions generate junctions that will present non-effective potential barriers, so that a parallel conduction through these non-active barriers will occur in varistor devices. This parallel conduction is responsible for the leakage current. In this case, the oxygen treatment cannot increase the potential barrier and density of states at the interface because the oxygen species will be consumed preferentially to eliminate the non-active potential barrier in regions with lower concentrations of segregated metal and enrich the precipitates with oxygen species.

It should be kept in mind that, for the model discussed in Refs. [1, 13, 14], the oxygen species (oxidation) enrichment of the grain boundary is related to the segregated metal atoms and precipitates, thus a balance between them is very important. Therefore, besides impoverishing the regions adjacent to them of metal atoms (during the sintering process), the precipitate phases will also compete for oxygen species during oxidizing treatments. In other words, the oxygen species are consumed preferentially by the precipitates at the triple points; this depletes the segregated (metal oxide) phase between two grain boundaries from oxygen, as a result of which the potential barrier will be decreased.

Our approach to the problem is in agreement with the complex plane analysis. Figure 4 shows the complex capacitance plane before and after thermal treatment in an oxygen-rich atmosphere, which was used as the best illustration of dispersion. From Fig. 4, one can see that the behavior before and after the oxygen-rich atmosphere is quite different, although the $\alpha$ values did not change significantly. The region of lower frequencies shows the presence of *dc* conduction, which contributes to the plot and represents the electrical response before the sample was subjected to the atmosphere-rich treatment (appearing as a slanted line that tends to increase parallel to the $C''$ axis in Fig. 4(a)). This response is similar to that presented in Ref. [13] for a $SnO_2$·CoO-based varistor at a temperature of 200°C. The contribution of conduction observed relates to non-active potential barriers in regions adjacent to the precipitate phases. The total electrical response appears to follow the Cole-Cole dielectric model with a resistance response parallel to it, representing the non-active potential barrier plus the conduction process through the barrier (which can be thermionic and/or tunneling conduction at lower potentials). Therefore, the paral-
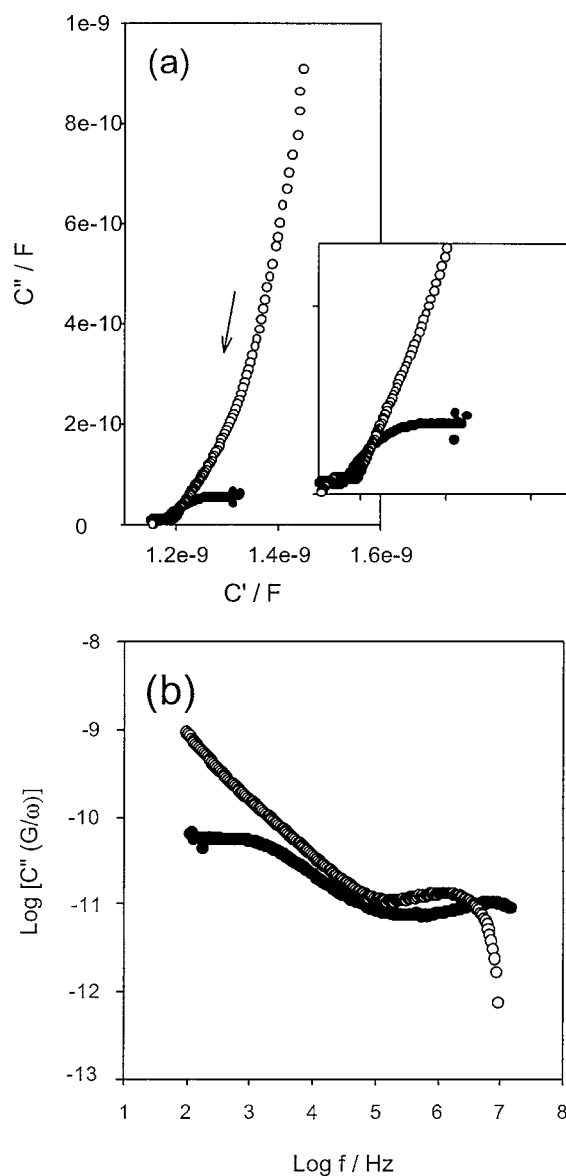


*Fig. 4.* (a) Complex capacitance behavior of the $SnO_2$·CoO-based system studied. The arrow point the direction of the increasing of the frequency. The inset shows the behavior at higher frequencies; (○) Response as sintered, and (●) after thermal treatment in an oxygen rich atmosphere. (b) $C'' = G/\omega$ response, showing the relaxation process associated with the trap states at the grain boundary of the system after thermal treatment in an oxygen-rich atmosphere. The as-sintered system shows a conduction process at lower frequencies.

lel process is connected to the higher value of leakage current observed.

On the other hand, the response after thermal treatment in an oxidizing atmosphere is completely

modified, particularly at lower frequencies. The response of the conduction mechanism is reduced (now the response is similar to that discussed in Ref. [13] at room temperature). The response of the high frequency region also changed to a different pattern. However, it changed to a complex behavior that can be attributed to the existence of two distinct relaxation processes (see reference [13] for details); the effect of the LRC resonance series response coupled with possible Cole-Cole dielectric relaxation. We do not intend to analyze this effect here, but will investigate it in a future study.

Our approach to the problem presented previously is also in agreement with the capacitance-voltage (C-V) analysis. The C-V analysis was done following the approach proposed in Ref. [13]. The C-V analysis, allied to the complex capacitance response was used to construct an appropriate Mott-Schottky behavior so that the parameters of the potential barrier were obtained, according to the following equation [13, 16].

$$\left(\frac{1}{C} - \frac{1}{2C_0}\right)^2 = \frac{2}{q\varepsilon_r\varepsilon_0 N_d}(\phi_b + V), \qquad (1)$$

where $q$ is the electron or elementary charge, $\varepsilon_r$ is the relative permittivity ($\sim$14), $\varepsilon_0$ is the permittivity of free space, $N_d$ is the donor concentration and $\phi_b$ is the barrier height of the system. $C_0$ and $C$ are the capacitance per unit area of a grain boundary biased, respectively, with zero and $V$ volts. The values of capacitance, taking from each biased-voltage, where obtained from the analysis of complex capacitance curve, taking the capacitance value of the high frequency intercept with x-axis (real axis) on the Fig. 4(a). Taking the linear relationship (not shown) from a plot of $(1/C - 1/2C_0)$ versus $V$, the values of $\phi_b$ and $N_d$ are easily obtained. The calculations must also to take into consideration the average number of grains between electrodes. Considering that the potential barrier is of back-to-back type, one obtains the following electrical neutrality condition:

$$N_{IS} = 2N_d\delta \qquad (2)$$

Combining (2) with Eq. (2) of Ref. [13], the following equation arises to the calculation of barrier width $\delta$:

$$\delta = \frac{1}{2}\left(\frac{2\varepsilon_0\varepsilon_r}{qN_D}\phi_b\right)^{1/2} \qquad (3)$$

The results from Mott-Schottky analysis are presented in Table 2. The calculations were made before

*Table 2.* $\phi_b$, $N_d$, $N_{IS}$ and barrier width ($\delta$) values for the SnO$_2$·CoO-based system studied before and after treatment in an rich-oxygen atmosphere. These calculations take into consideration the average number of grains between electrodes.

|  | $\phi_b$/V | $\delta$/nm | $N_d$ ($10^{24}$)/m$^{-3}$ | $N_{IS}$ ($10^{17}$)/m$^{-2}$ |
|---|---|---|---|---|
| As sintered | 1.09 | 14.8 | 2.5 | 0.74 |
| After O$_2$ rich atmosphere treatment | 1.12 | 15.2 | 2.3 | 0.70 |

and after thermal treatment in an oxidizing atmosphere. The value of frequency-dependence capacitance, used in conjunction with the sample's mean grain size values, reflects the average Mott-Schottky response of any junction within the device. Therefore, the influence of the microstructure must be considered carefully, because parallel effects may lead to misinterpretations of the results obtained.

Therefore, as indicated by the results in Table 1, the values of potential barrier height ($\phi_b$), donor concentration ($N_d$) and density of state at the interface ($N_{IS}$) did not change within experimental error. This means that the oxygen treatment did not influence (improve) the existing active barrier, but only converted a percentage of non-active barriers into active ones, decreasing the leakage current without substantially improving the system's nonohmic properties. This effect is expected for SnO$_2$ devices with higher concentrations of precipitate phase at triple points of the grain boundary.

## Conclusions

Microstructural heterogeneities, such as an excess of precipitate phase at triple points in the grain boundary region, may be deleterious to the nonohmic properties of SnO$_2$-based varistor devices. Excess precipitates may have the effect of causing high leakage current values. From this standpoint, thermal treatments in an oxygen atmosphere may decrease the leakage current, but cannot increase the varistor's nonlinear coefficient values.

## Acknowledgments

## References

1. P.R. Bueno, E.R. Leite, M.M. Oliveira, M.O. Orlandi, and E. Longo, *Applied Physics Letter*, **79**, 48 (2001).
2. M.R. Cassia-Santos, P.R. Bueno, E. Longo, and J.A. Varela, *Journal of the European Ceramic Society*, **21**, 161 (2000).
3. E.R. Leite, A.M. Nascimento, P.R. Bueno, E. Longo, and J.A. Varela, *Journal of Materials Science: Materials in Electronics*, **10**, 321 (1999).
4. S.A. Pianaro, P.R. Bueno, E. Longo, and J.A. Varela, *Journal of Materials Science Letters*, **14**, 692 (1995).
5. S.A. Pianaro, P.R. Bueno, P. Olivi, and E. Longo, *Journal of Materials Science Letters*, **16**, 634 (1997).
6. S.A. Pianaro, P.R. Bueno, P. Olivi, E. Longo, and J.A. Varela, *Journal of Materials Science: Materials in Electronics*, **9**, 158 (1998).
7. S.A. Pianaro, P.R. Bueno, E. Longo, and J.A. Varela, *Ceramics International*, **25**, 1 (1999).
8. M.S. Castro and C.M. Aldao, *Journal of European Ceramic Society*, **18**, 2233 (1998).
9. J.A. Cerri, E.R. Leite, D. Gouvea, and E. Longo, *Journal American Ceramic Society*, **79**, 799 (1996).
10. J.A. Varela, J.A. Cerri, E.R. Leite, E. Longo, M. Shamsuzzoha, and R.C. Bradt, *Ceramics International*, **25** (1999).
11. Y.J. Wang, J.F. Wang, C.P. Li, H.C. Chen, W.B. Su, W.L. Zhong, P.L. Zhang, and L.Y. Zhao, *The European Physical Journal Applied Physics*, **11**, 155 (2000).
12. W. Yongjun, W. Jinfeng, C. Hongcun, Z. Weilie, Z. Peilin, D. Huomin, and Z. Lianyi, *Journal Physical D: Applied Physics*, **33**, 96 (2000).
13. P.R. Bueno, M.R. Cassia-Santos, E.R. Leite, E. Longo, J. Bisquert, G. Garcia-Belmont, and F. Fabregat-Santiago, *Journal of Applied Physics*, **88**, 6545 (2000).
14. P.R. Bueno, M.M. Oliveira, W.K. Bacelar-Junior, E.R. Leite, E. Longo, G. Garcia-Belmont, and J. Bisquert, *Journal of Applied Physics*, **91**, 6007 (2002).
15. M.M. Oliveira, P.R. Bueno, M.R. Cassia-Santos, E. Longo, and J.A. Varela, *Journal of the European Ceramic Society*, **21**, 1179 (2001).
16. K. Mukae, K. Tsuda, and I. Nagasawa, *Journal of Applied Physics*, **50**, 4475 (1979).